Table 1: Comparison of strain capability [4, 5, 6 and 20]

Material	Saturation strain in [ppm]	Curie temperature in [K]
Ni	-50	630
Fe	-14	1040
Fe_3O_4	60	860
Terfenol-D	2000	650
$Tb_{0.5}Zn_{0.5}$	5500	180
$Tb_{0.5}Dy_xZn$	5000	200

Table 2: Typical layouts in comparison similar to [7, 8]

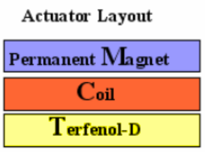 ***Typical actuator features***	**TC** 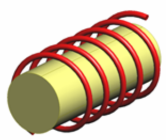	**TCM** 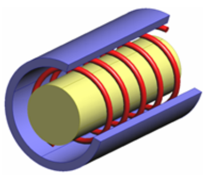	**TMC** 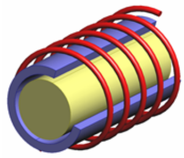	**MTC** 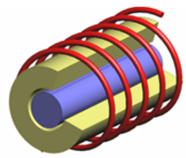
Magnetic bias with	DC coil	Permanent magnets		
Magnetic bias level	Low	Medium	Medium, high	High
Terfenol-D shape	Rod, bar	Rod	Rod	Hollow rod
Structure	Simple	Medium	Medium	Complex
Field inhomogeneity	Low	Low	Medium	High

Table 3: "MS"-actuator key data

"MS"-actuator, 3D CAD cut view	Actuator key data	Experimental results
Actuator 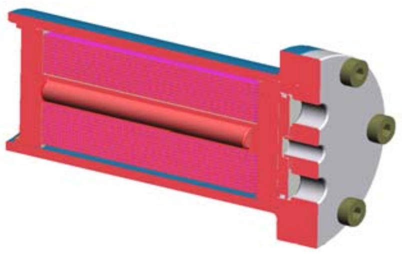	Actuator coil: -950 turns, 1.5Ohm -wire diameter of 1.12mm Terfenol-D shaft: -shaft diameter of 8mm -shaft length 67.5mm	Optimized pre-stress: 12MPa (600N pre-load) Strain capability: 0.065mm @10 A (1000ppm @ 105 kA/m) Blocked force: > 4500N

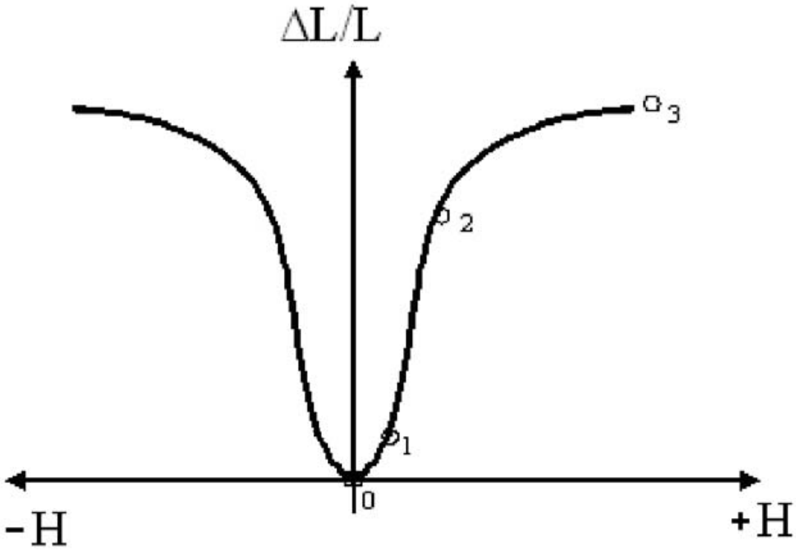

Fig.1: Strain versus magnetic field

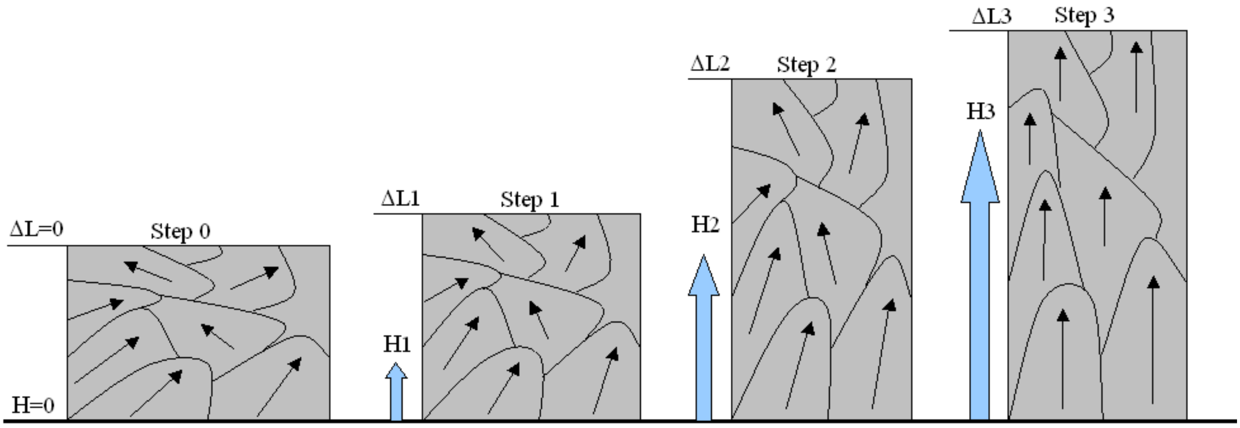

Fig. 2: “MS”-effect, schematically

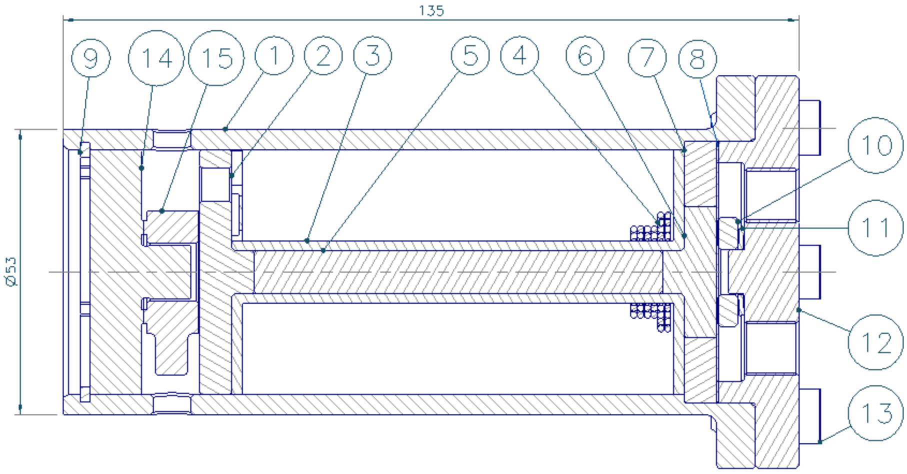

BoM #	Part #	Title
1	700.001	Housing
2	700.002	Cover LH
3	700.003	Coil bobbin
4	700.004	Coil
5	700.005	Terfenol-D shaft
6	700.006	Piston
7	700.007	Cover RH piston
8	700.008	Membrane
9	700.009	Circlip
10	700.010	Spring cover
11	700.011	Spring
12	700.012	Cover RH
13	700.013	Screw
14	701.015	Force sensor
15	702.016	Sensor cover

Fig. 3: Cross-section of the actuator used in the study

TERFENOL-D PHYSICAL PROPERTIES	
Nominal Composition	$Tb_{0.3}Dy_{0.7}Fe_{1.92}$
Mechanical Properties	
Young's Modulus	25-35 GPA
Sound Speed	1640-1940 m/s
Tensile Strength	28 Mpa
Compressive Strength	700 Mpa
Thermal Properties	
Coefficient of Thermal Expansion	12ppm/°C
Specific Heat	0.35kJ/kg-K
Thermal Conductivity	13.5 W/m-k
Electrical Properties	
Resistivity	58 x 10-8 O-m
Curie Temperature	380 °C
Magnetostrictive Properties	
Strain (estimated linear)	800-1200ppm
Energy Density	14-25 kJ/ m^3
Magnetomechanical Properties	
Relative Permeability	3-10
Coupling Factor	0.75

Fig. 4: Supplier characteristic and specification for Terfenol-D shaft [4]

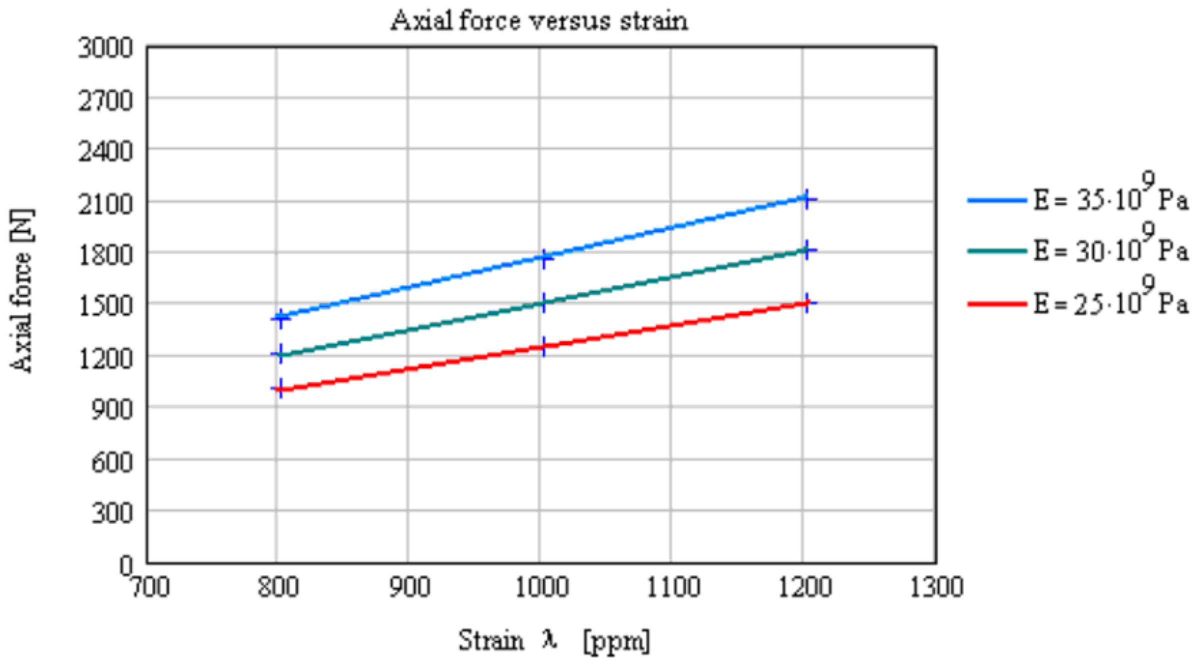

Fig. 5: Axial force versus strain and Young’s modulus E as parameter

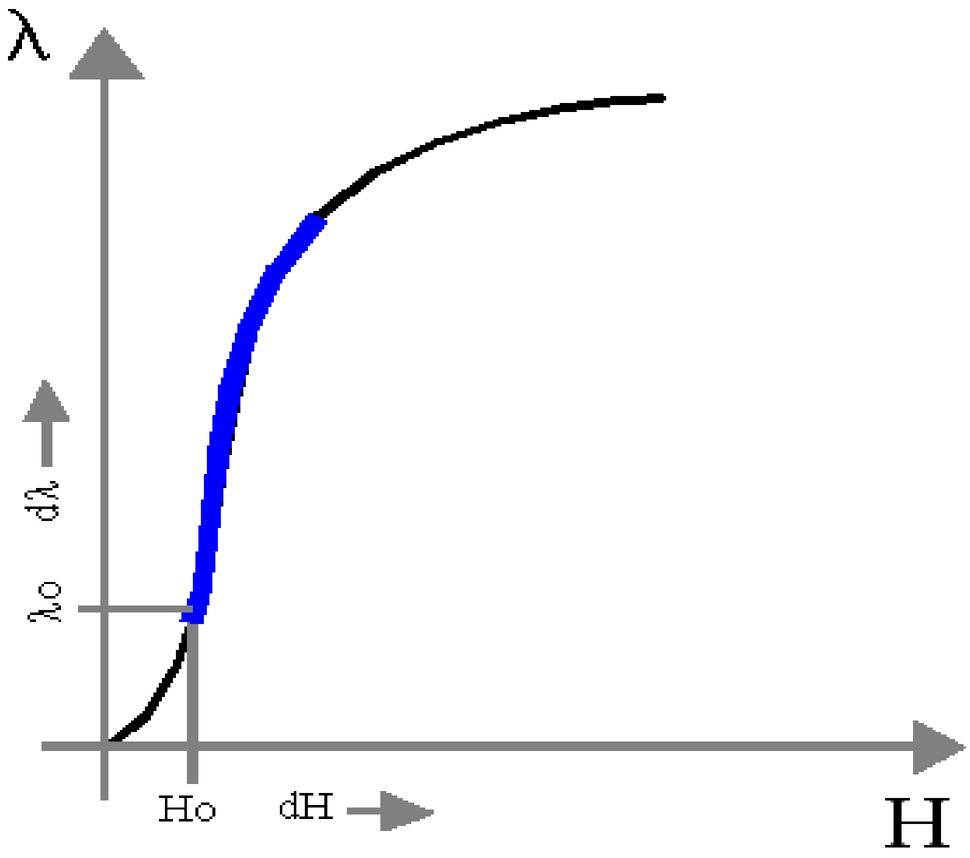

Fig.6: Typical optimization with magnetic bias

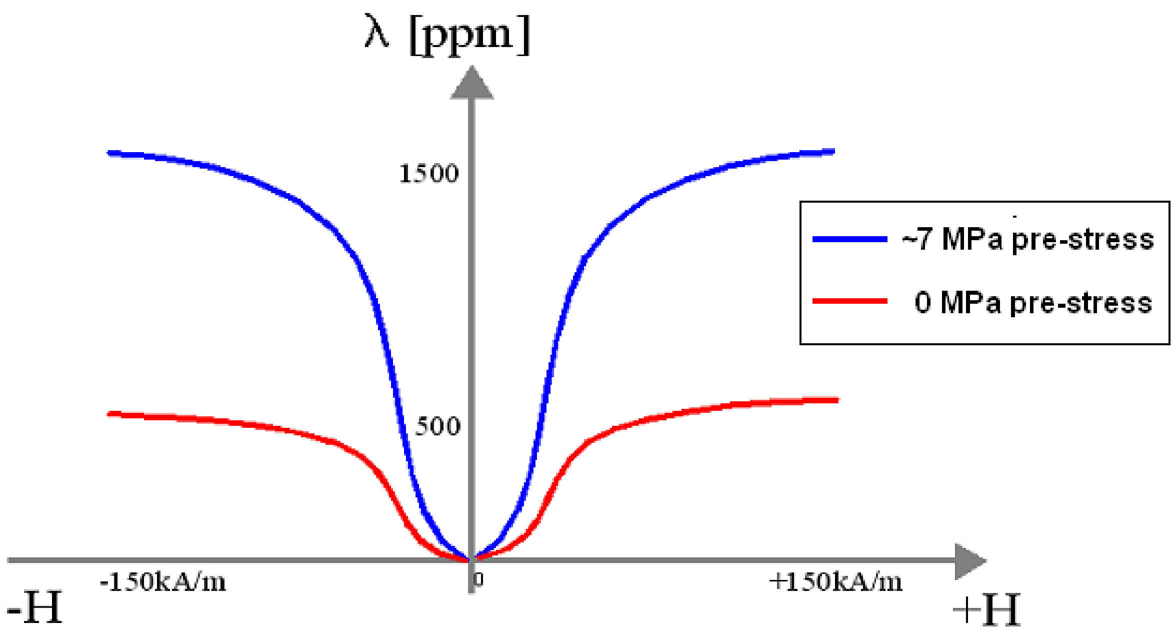

Fig.7: Typical optimization with mechanic bias [similar to 9, 10 and 11]

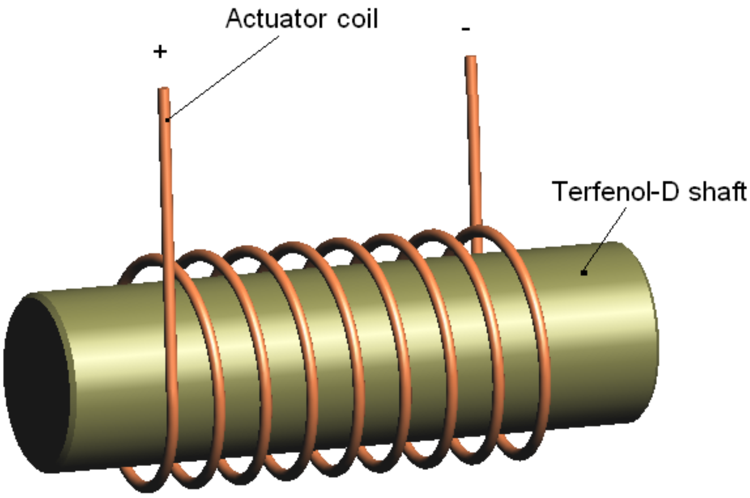

Fig. 8: TC-Layout of the actuator coil

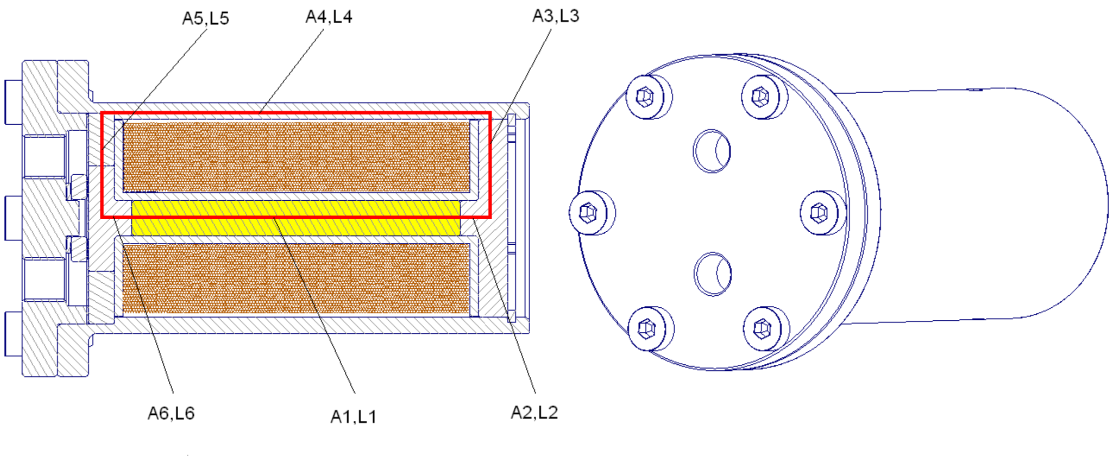

Fig. 9: Magnetic path through the actuator

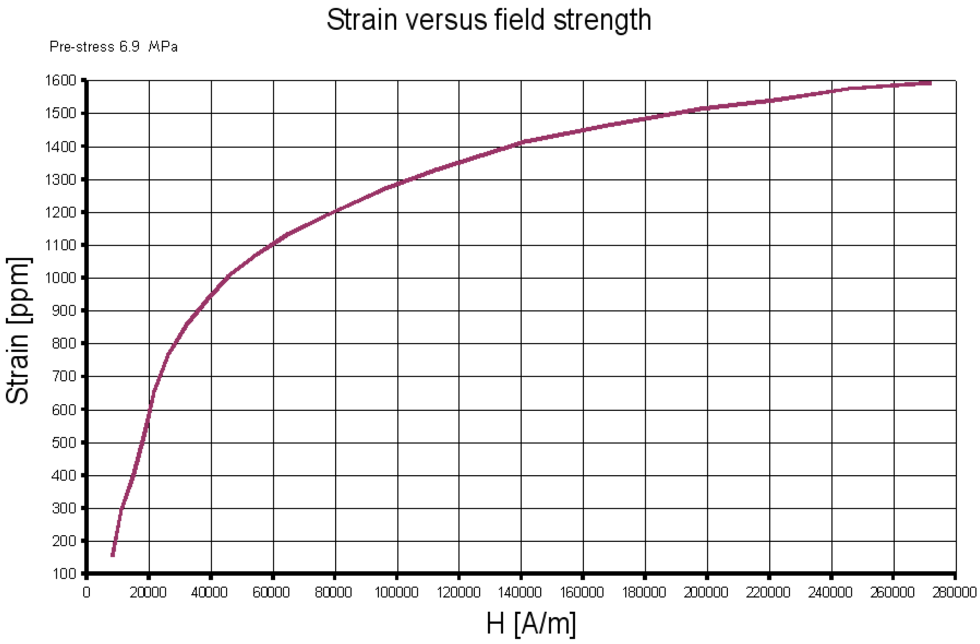

H [A/m]	Strain [ppm]
8105	150
10977	296
14806	393
18636	532
21507	655
26294	767
32038	859
38739	936
45440	1005
54056	1067
64586	1133
77031	1190
96177	1271
112451	1329
141170	1414
167975	1464
197651	1514
221584	1541
245517	1576
272321	1595

Fig. 10: Strain versus applied magnetic field intensity (A/m) [4]

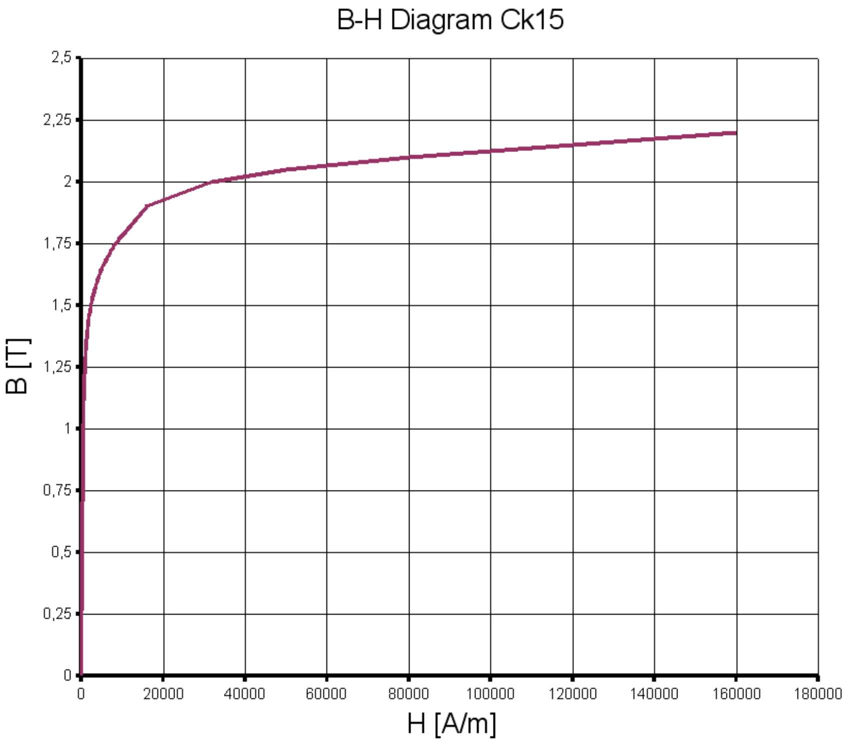

H	B	µ	µr
0	0	-	-
100	0,26	2,62E-003	2087
200	0,5	2,48E-003	1976
300	0,7	2,35E-003	1868
400	0,89	2,21E-003	1763
500	1,02	2,04E-003	1624
600	1,11	1,86E-003	1476
700	1,17	1,68E-003	1336
800	1,22	1,53E-003	1215
900	1,26	1,40E-003	1112
1000	1,29	1,29E-003	1026
1100	1,32	1,20E-003	952
1200	1,34	1,12E-003	889
1300	1,36	1,05E-003	834
1400	1,38	9,86E-004	785
1500	1,4	9,32E-004	742
1600	1,41	8,84E-004	703
1700	1,43	8,40E-004	669
1800	1,44	8,01E-004	637
1900	1,45	7,65E-004	609
2000	1,47	7,33E-004	583
2400	1,5	6,27E-004	499
2800	1,54	5,49E-004	436
3200	1,56	4,88E-004	388
3600	1,59	4,40E-004	350
4000	1,61	4,01E-004	319
4400	1,62	3,69E-004	294
4800	1,64	3,42E-004	272
5200	1,66	3,18E-004	253
5600	1,67	2,98E-004	237
6000	1,68	2,80E-004	223
6400	1,7	2,65E-004	211
6800	1,71	2,51E-004	200
7200	1,72	2,39E-004	190
7600	1,73	2,28E-004	181
8000	1,74	2,17E-004	173
8400	1,75	2,08E-004	166
8800	1,76	2,00E-004	159
9200	1,77	1,92E-004	153
9600	1,78	1,85E-004	147
16000	1,9	1,19E-004	95
32000	2	6,25E-005	50
50000	2,05	4,10E-005	33
80000	2,1	2,63E-005	21
160000	2,2	1,38E-005	11

Fig. 11: B-H diagram of Ck15 with measurement data

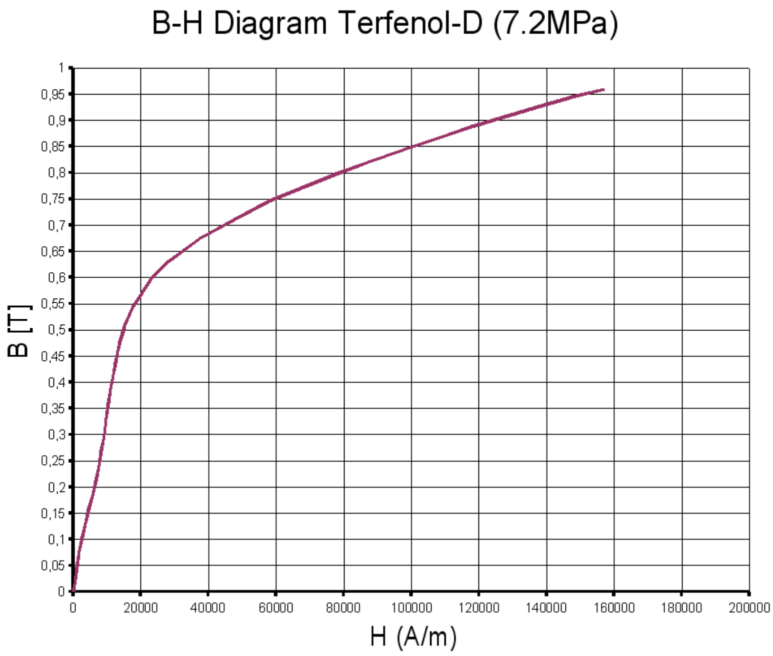

H (A/m)	B (Tesla)	µ	µ(r)
0	0	-	-
418	0,01	3,39E-005	26,94
1115	0,05	4,24E-005	33,72
1811	0,08	4,27E-005	33,95
2740	0,11	3,84E-005	30,55
3669	0,13	3,57E-005	28,43
4598	0,16	3,41E-005	27,16
5759	0,18	3,17E-005	25,25
6687	0,21	3,15E-005	25,06
7616	0,24	3,15E-005	25,03
8313	0,27	3,24E-005	25,81
9242	0,3	3,24E-005	25,79
9706	0,33	3,41E-005	27,11
10403	0,36	3,46E-005	27,52
11099	0,39	3,49E-005	27,8
11796	0,41	3,51E-005	27,91
12493	0,44	3,50E-005	27,88
13189	0,46	3,48E-005	27,67
13886	0,48	3,44E-005	27,37
14582	0,49	3,39E-005	26,98
15279	0,51	3,33E-005	26,52
17601	0,54	3,09E-005	24,62
22942	0,6	2,61E-005	20,73
28283	0,63	2,23E-005	17,74
37571	0,67	1,80E-005	14,29
47788	0,71	1,49E-005	11,83
58005	0,75	1,29E-005	10,24
67757	0,77	1,14E-005	9,07
77742	0,8	1,03E-005	8,16
87495	0,82	9,38E-006	7,46
97944	0,84	8,62E-006	6,86
107696	0,87	8,04E-006	6,39
117913	0,89	7,53E-006	5,99
127666	0,91	7,10E-006	5,65
137651	0,93	6,73E-006	5,35
147636	0,94	6,40E-006	5,09
157156	0,96	6,11E-006	4,86

Fig. 12: B-H diagram of Terfenol-D with measurement data [4]

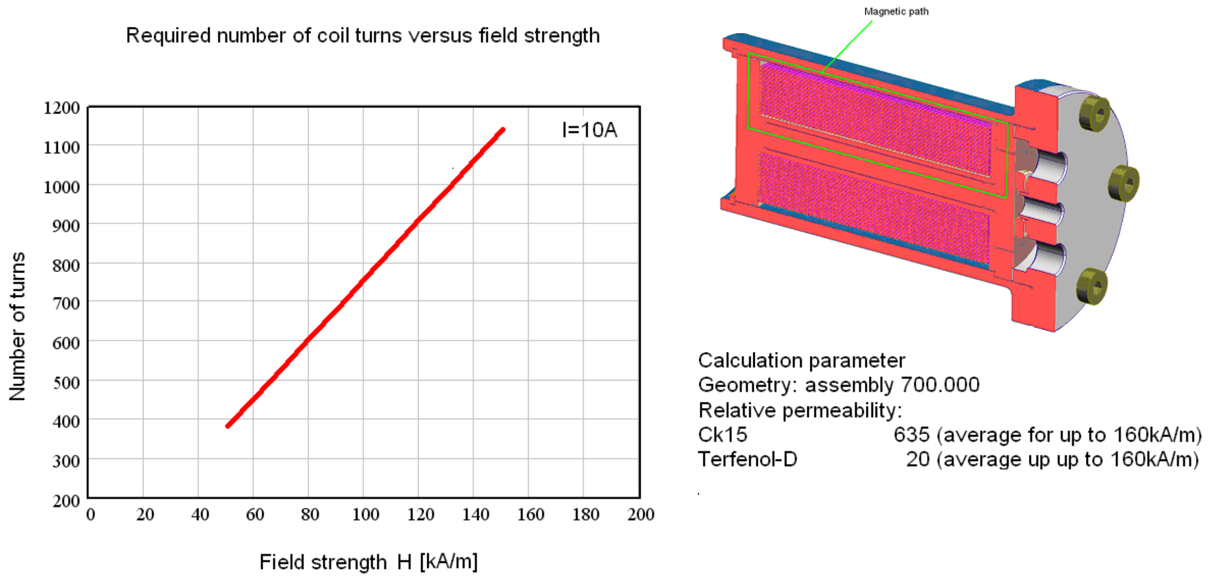

Fig. 13: Number of turns versus achievable magnetic field strength

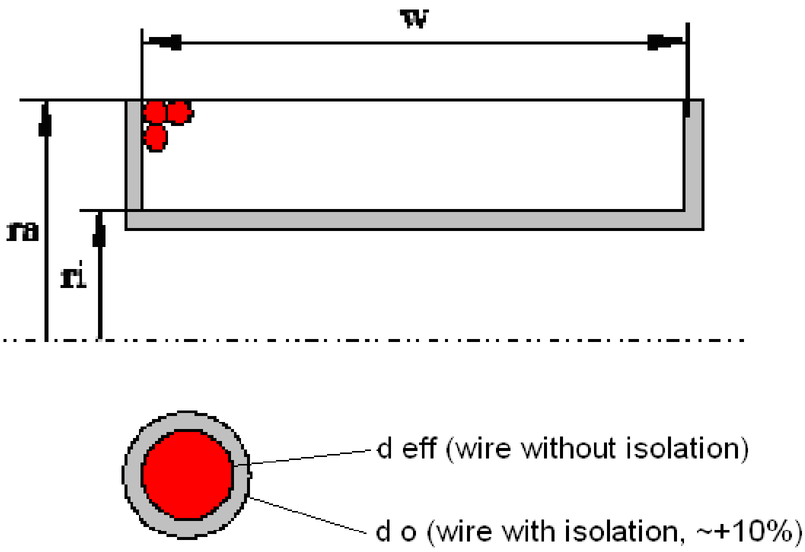

Fig. 14: Air coil geometry

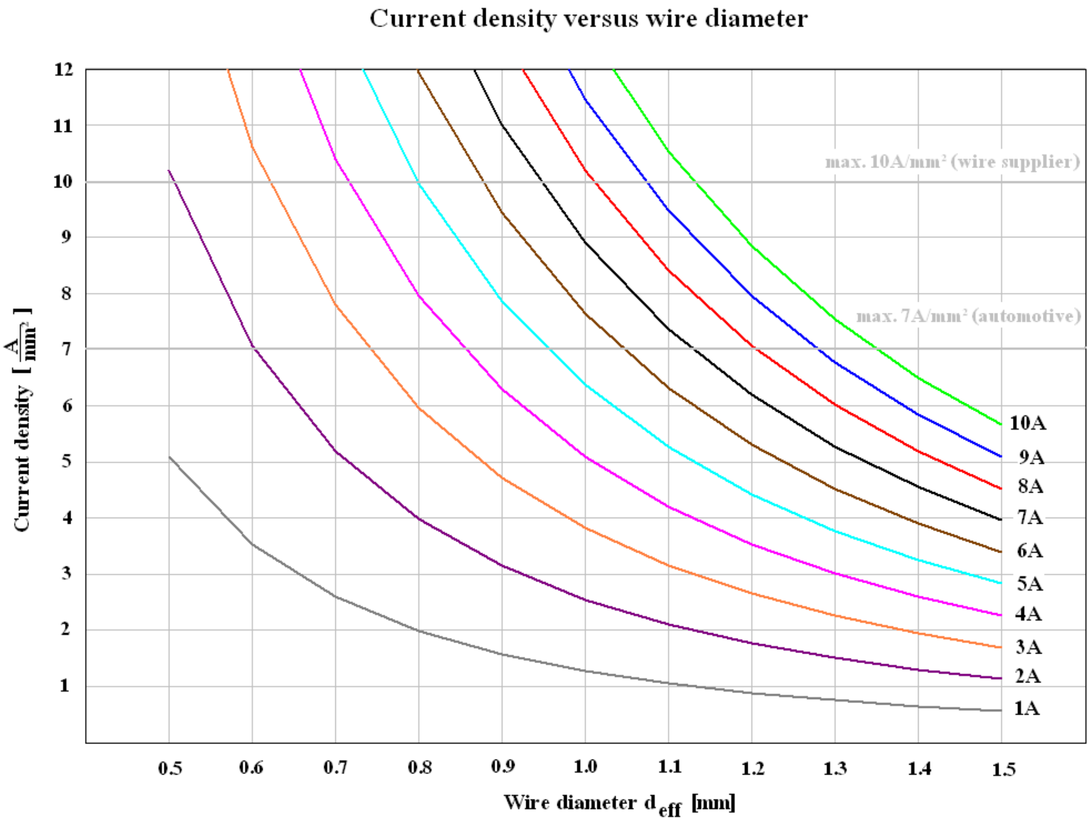

Fig. 15: Current density versus wire diameter with current as parameter

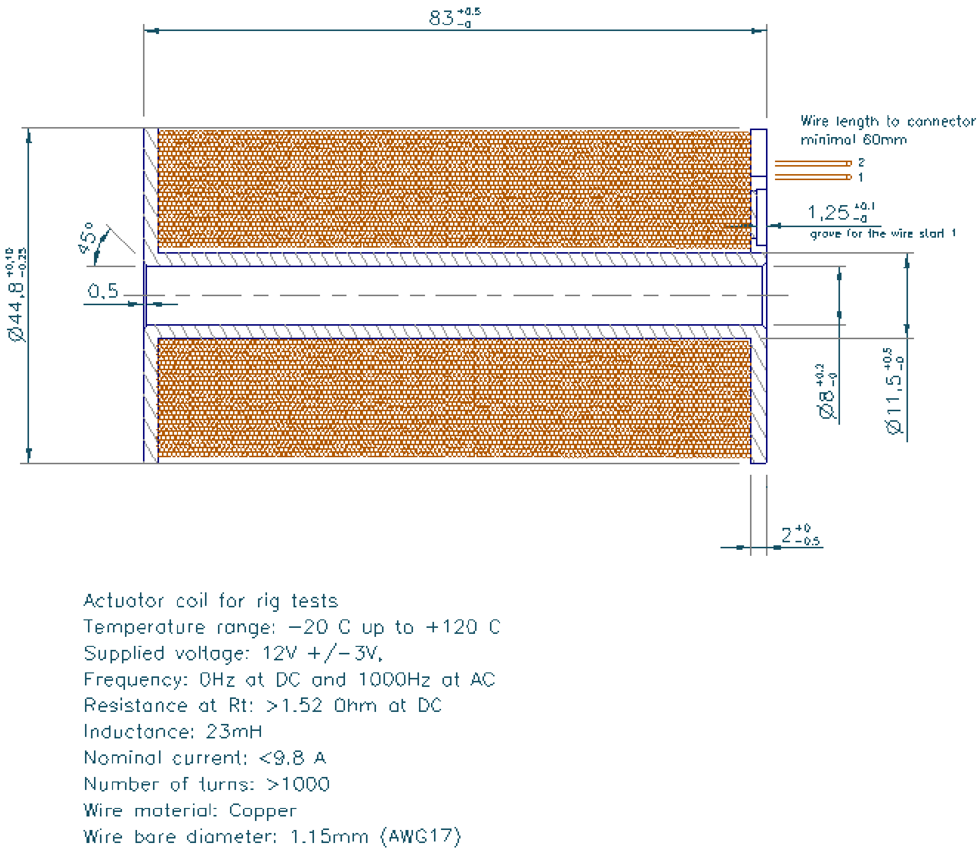

Fig. 16: Geometry and coil specification of the magnetostrictive actuator

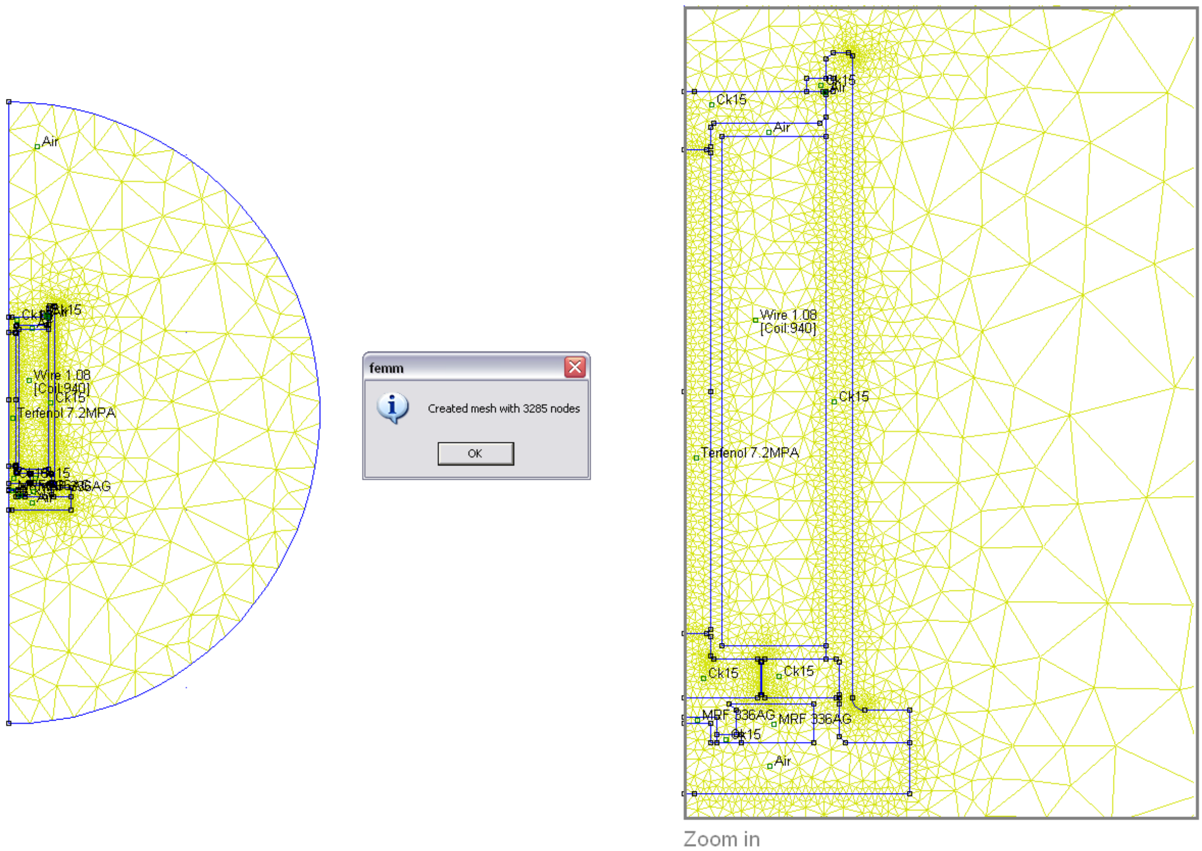

Fig. 17: Meshed actuator with FEMM

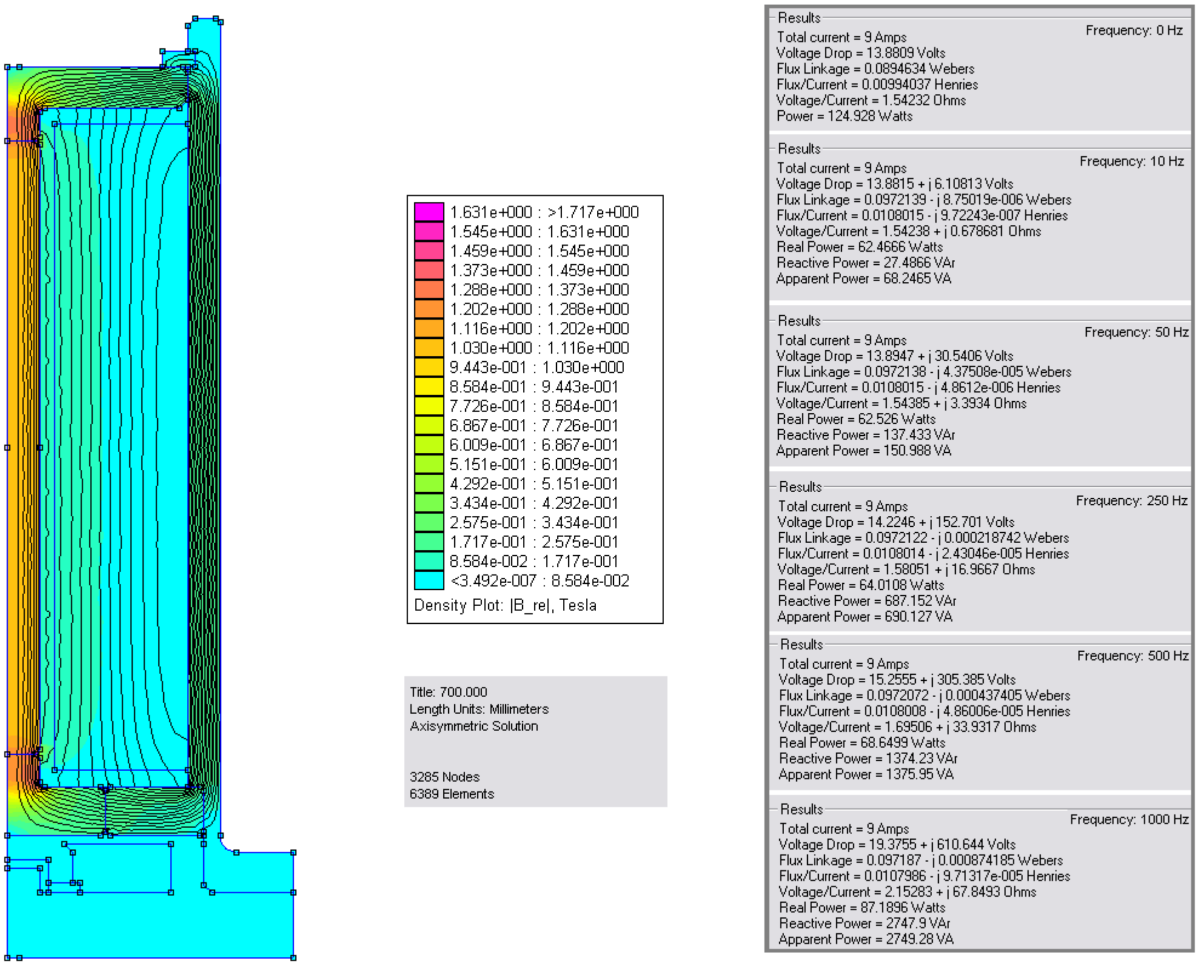

Fig. 18: FEMM Magnetic Field Density plot B (Tesla) in the actuator

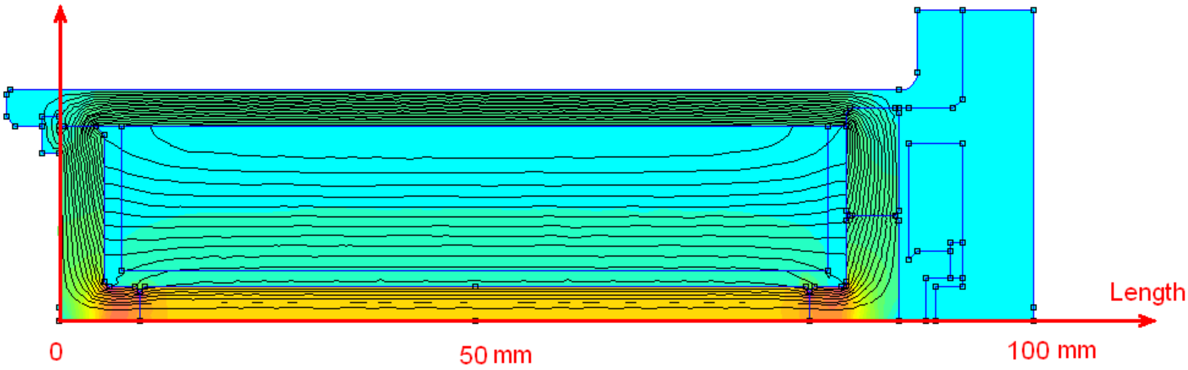

Fig. 19: Reference figure of the actuator plots of B (Tesla) and H (A/m)

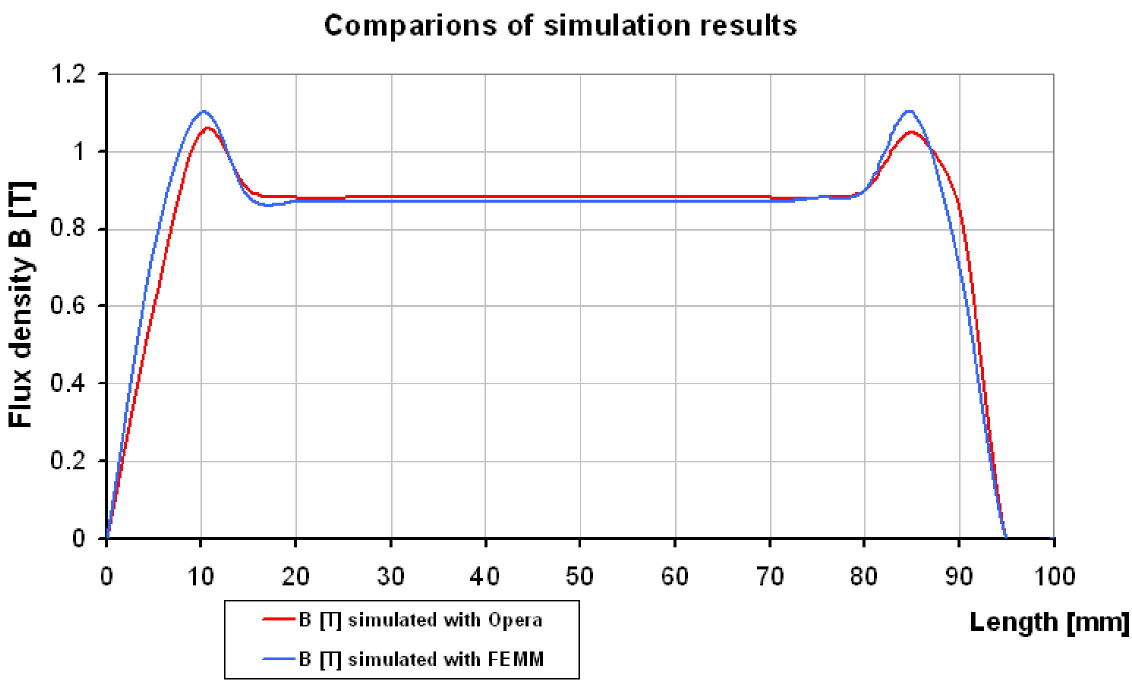

Fig. 20: Comparison of simulation results regarding flux density B (T)

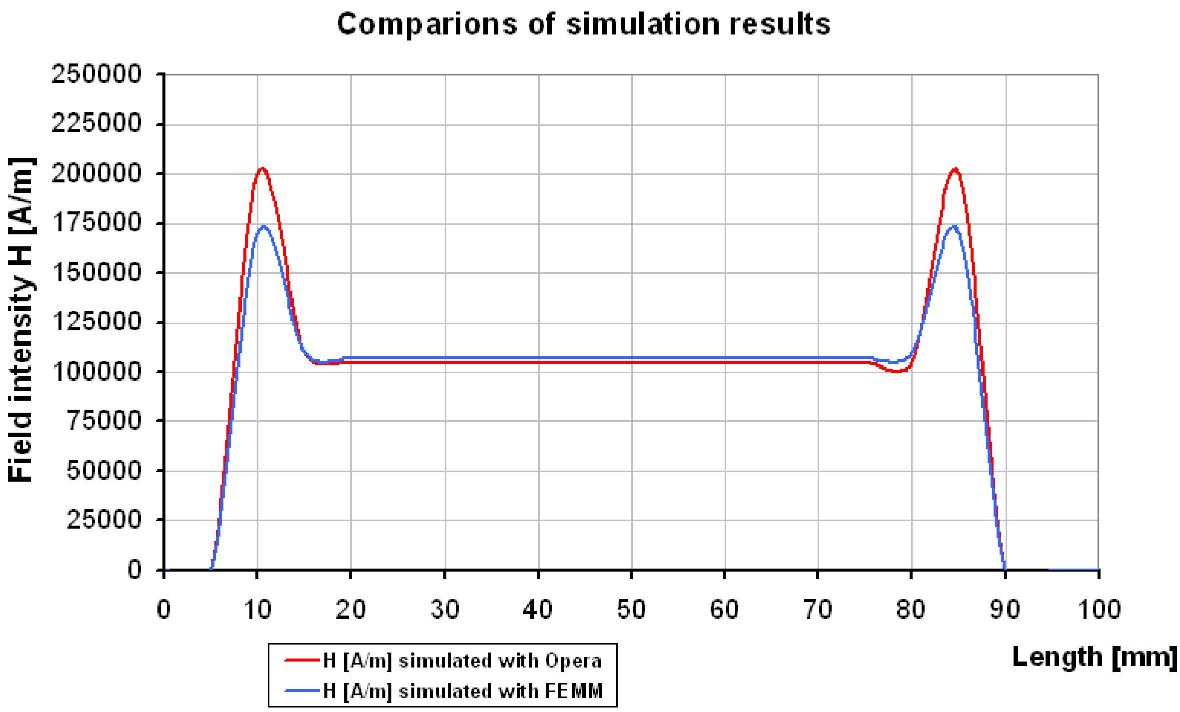

Fig. 21: Comparison of simulation results regarding field intensity H (A/m)

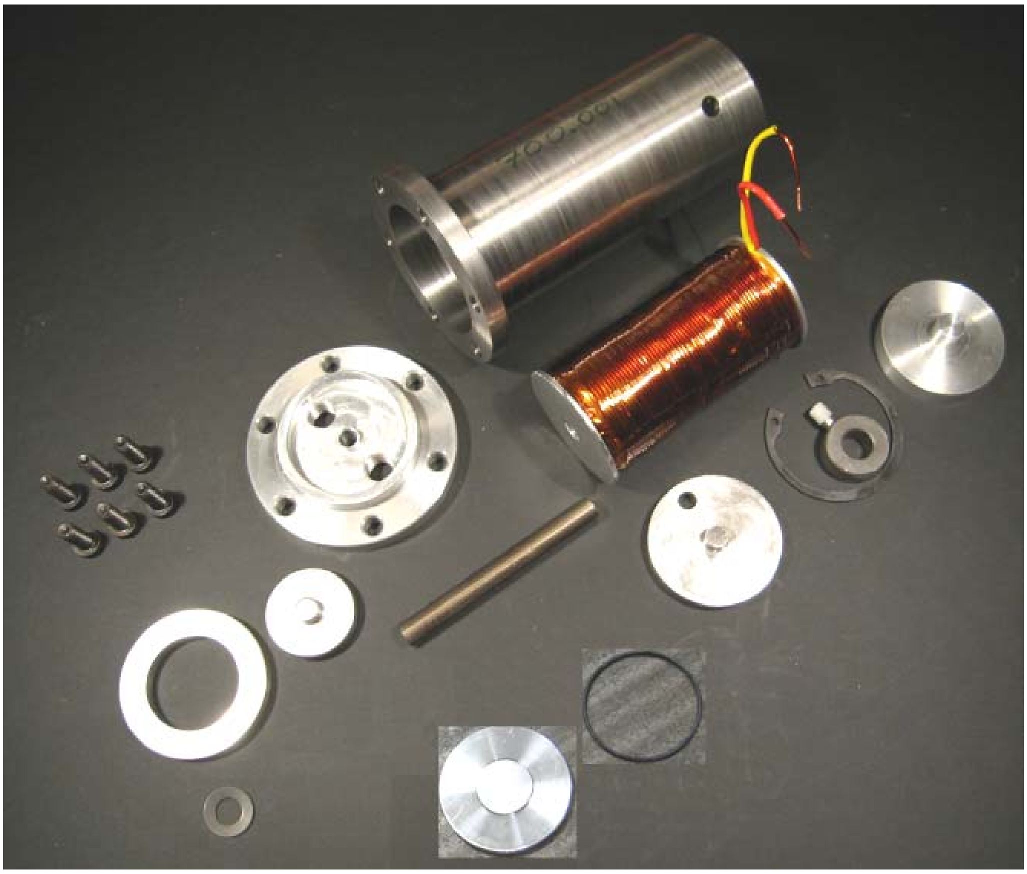

Fig. 22: Picture from “MS”-actuator assembly

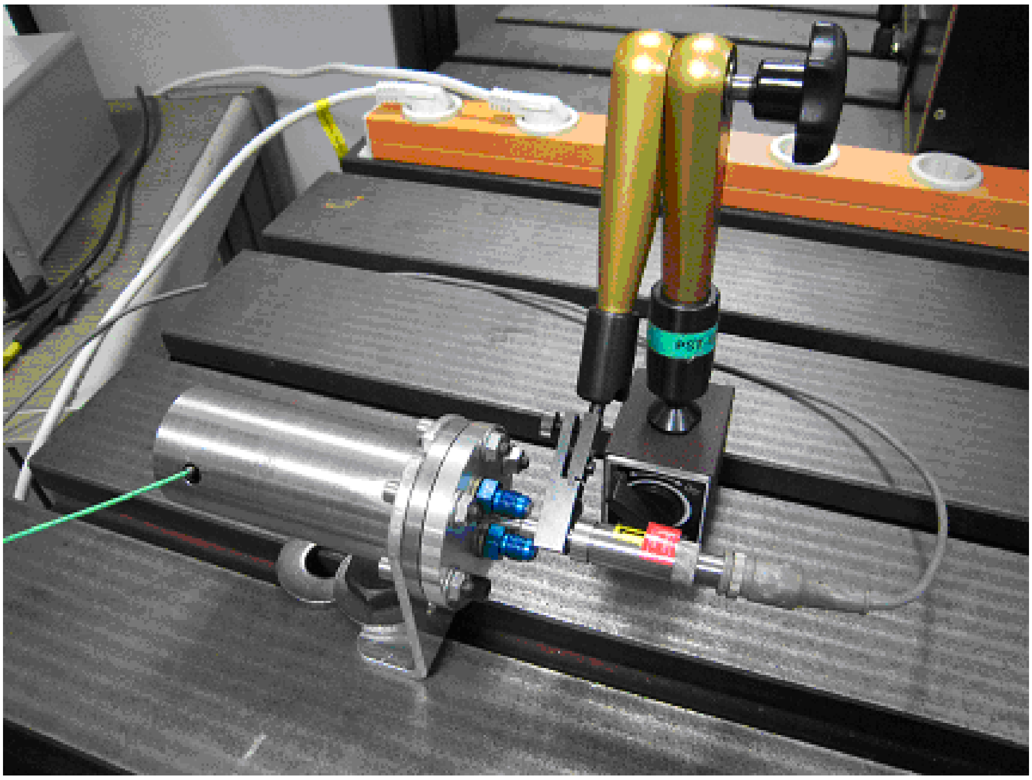

Fig. 23: Actuator assembly for performance measurements

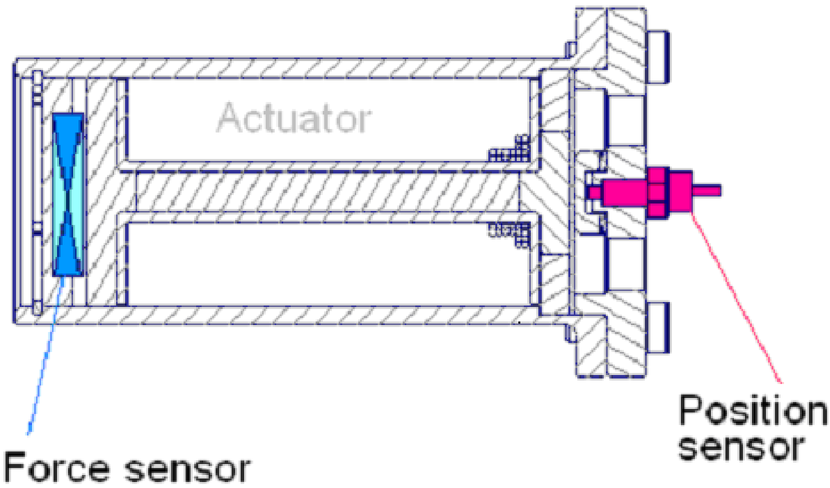

Fig. 24: Actuator assembly cross section for performance measurements

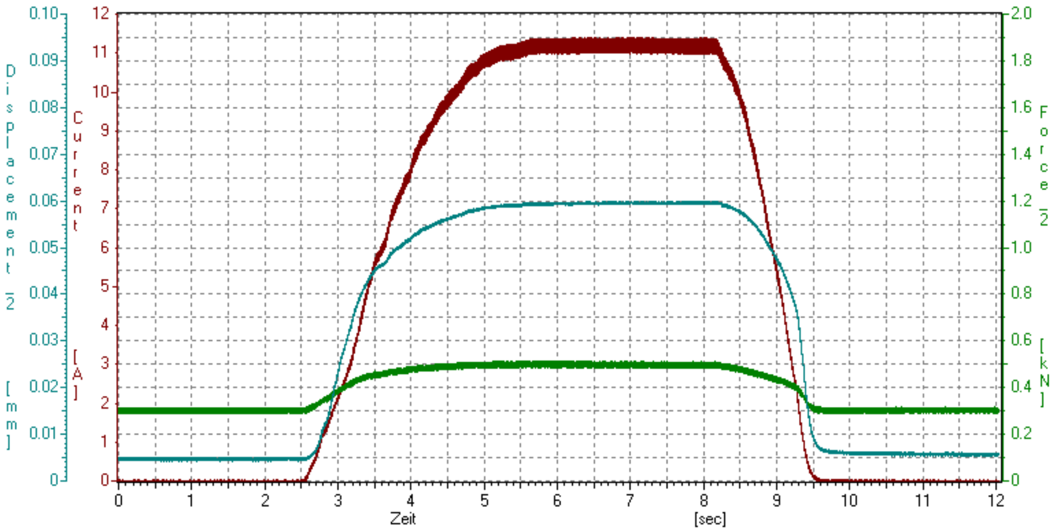

Fig. 25: Displacement, current and axial force versus time with 300 N pre-load

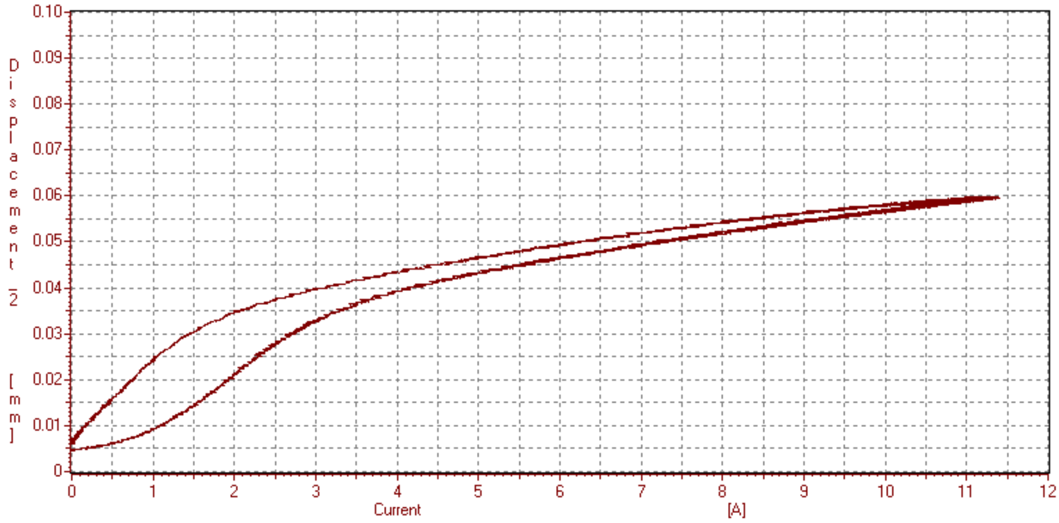

Fig. 26: Displacement versus current with 300 N

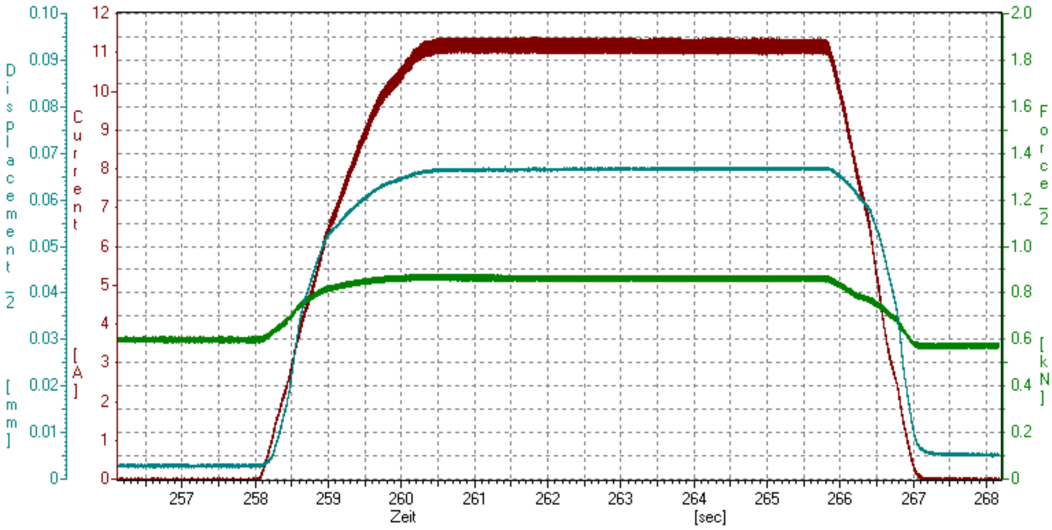

Fig. 27: Displacement, current and axial force versus time with 600 N pre-load

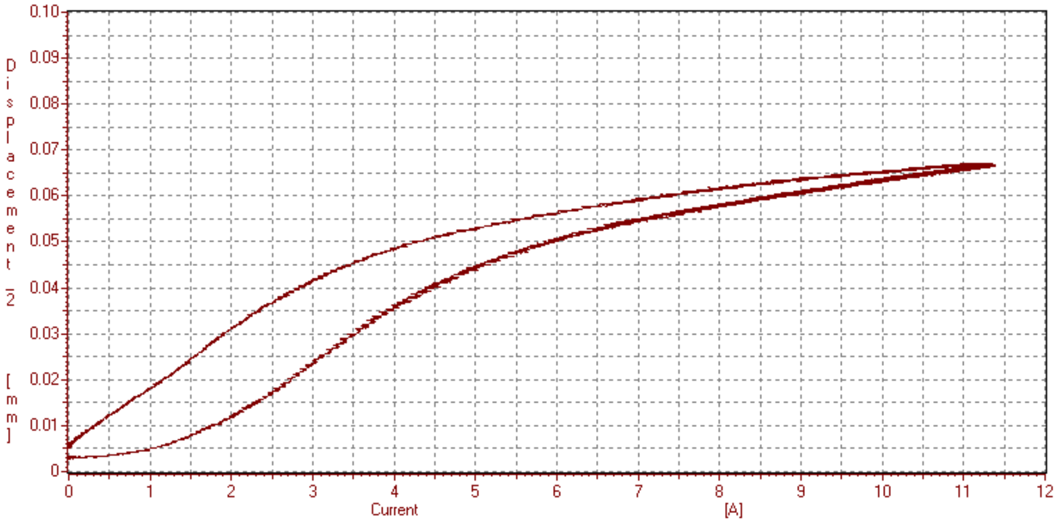

Fig. 28: Displacement versus current with 600 N

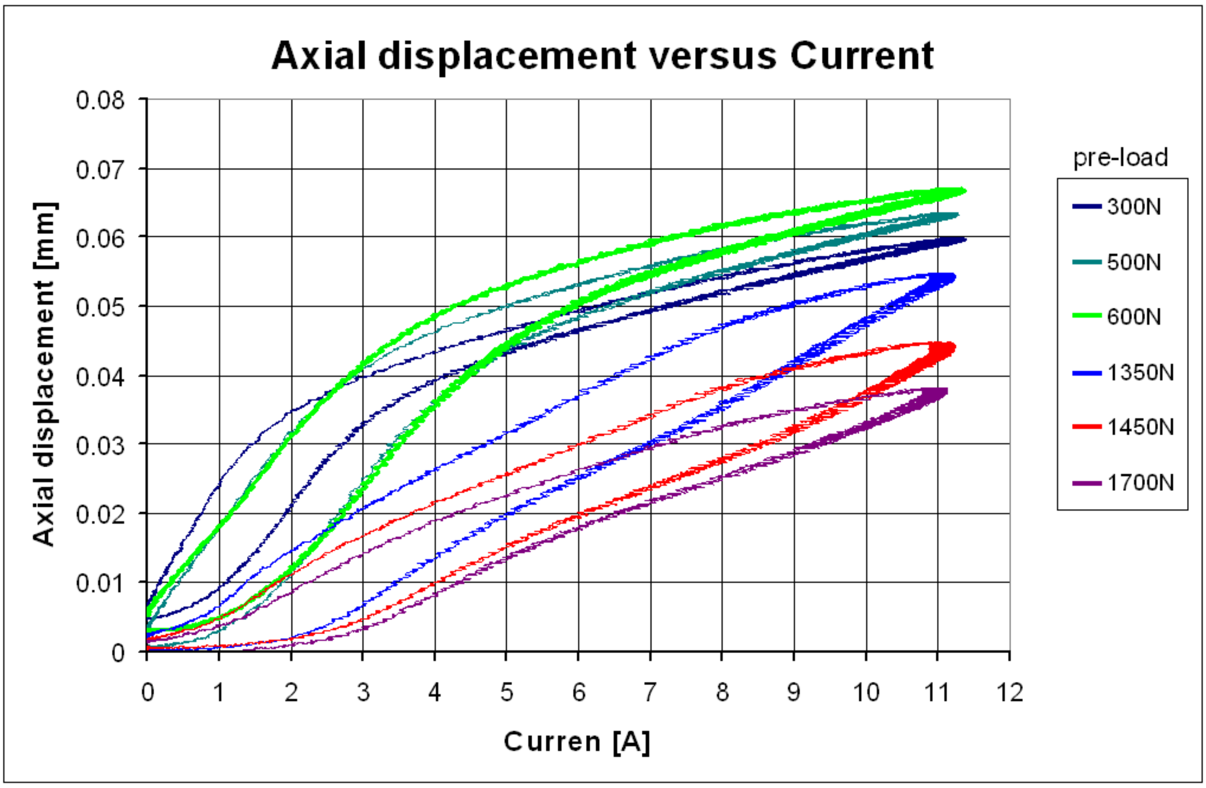

Fig. 29: Optimization of achievable strain with various pre-load

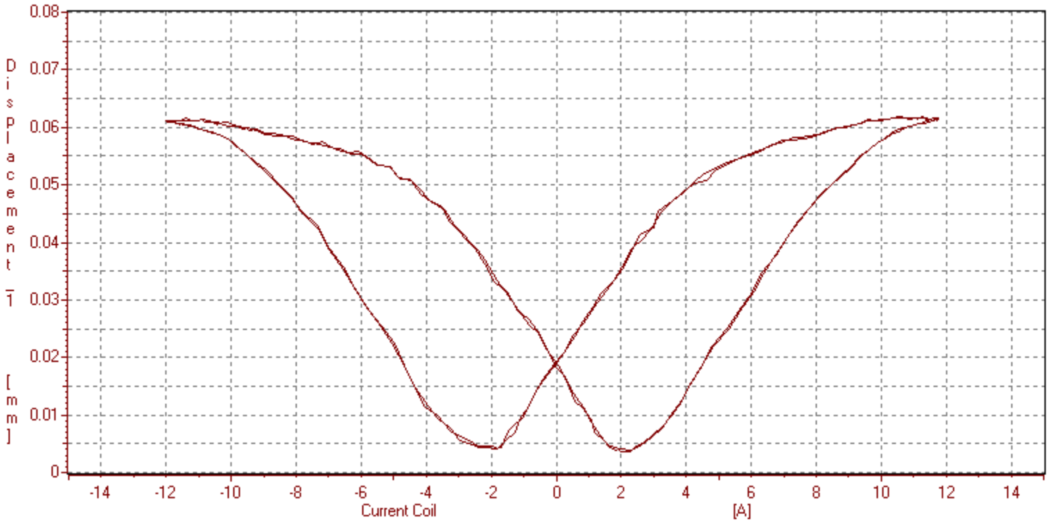

Fig. 30: Butterfly-curve at 550N pre-load & 20Hz sinusoidal power input

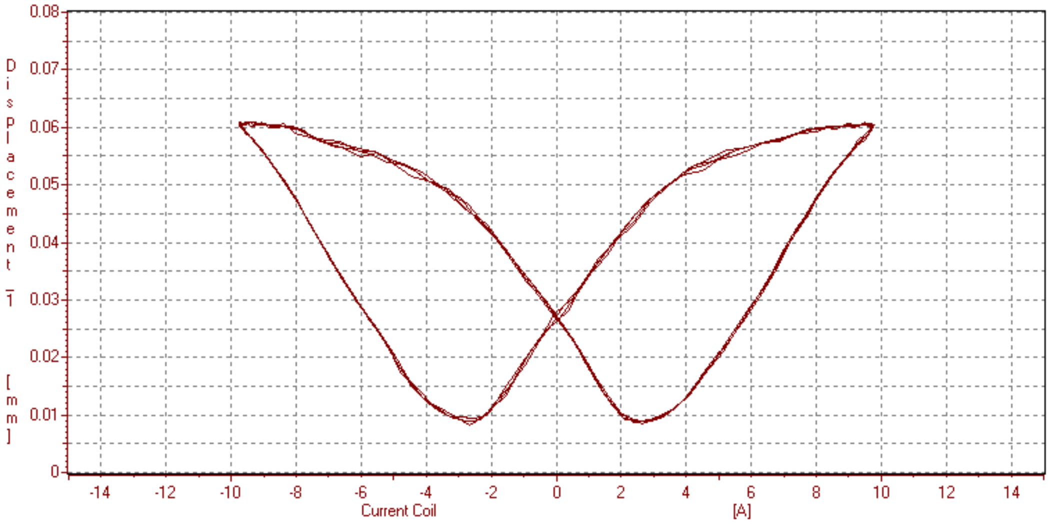

Fig. 31: Butterfly-curve at 550N pre-load & at 40Hz sinusoidal power input

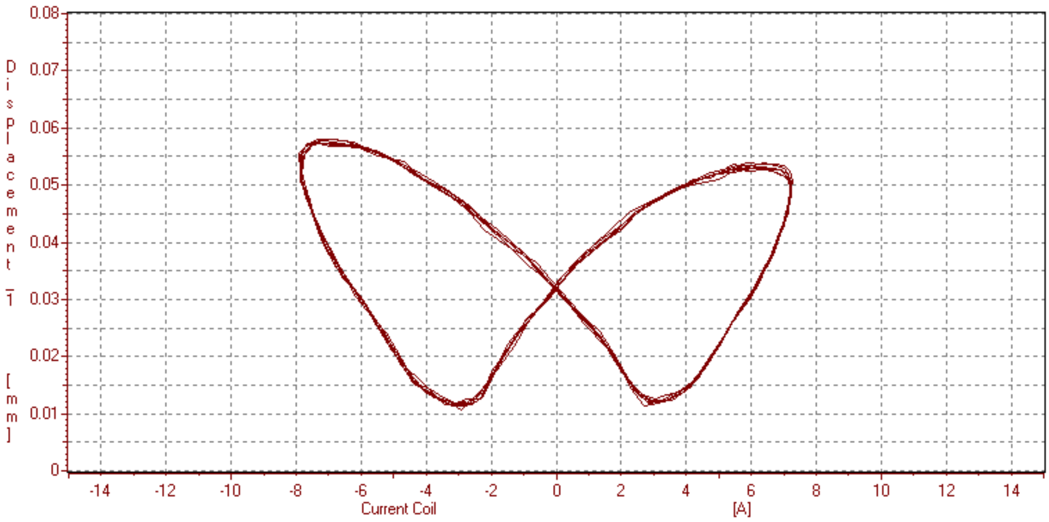

Fig. 32: Butterfly-curve at 550N pre-load & at 60Hz sinusoidal power input

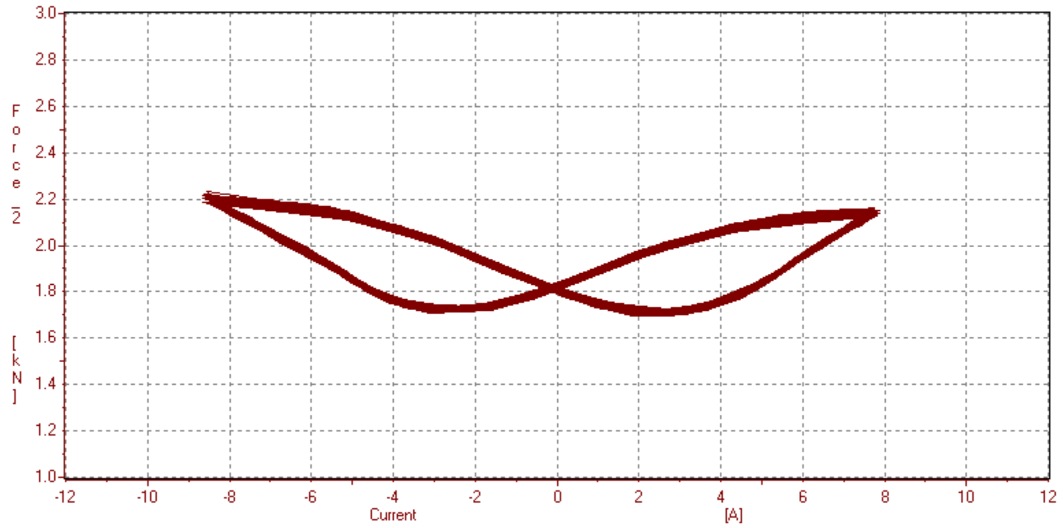

Fig. 33: Butterfly-curves, force versus current at medium pre-stress

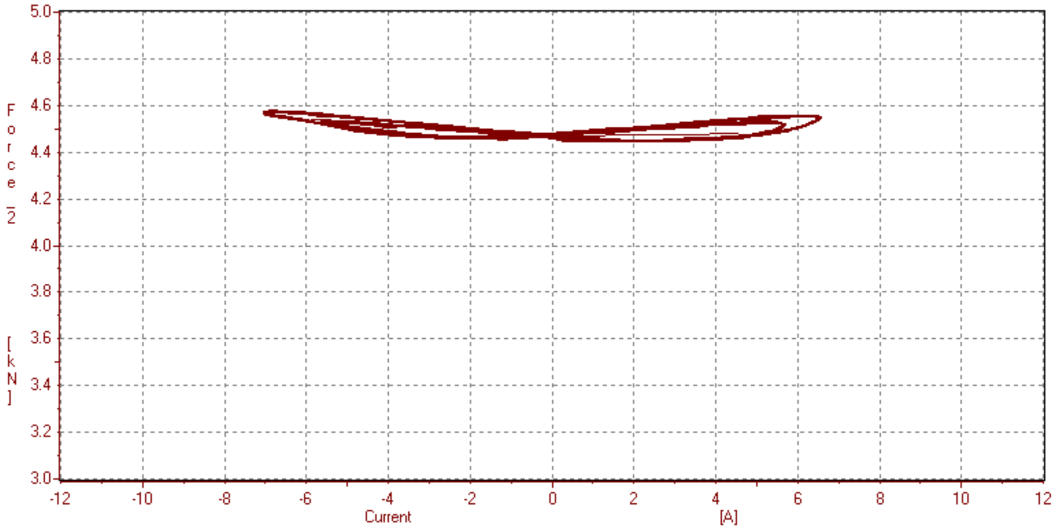

Fig. 34: Butterfly-curves, force versus current, at high pre-stress